

First principles prediction of the elastic, electronic and optical properties of Sn_3X_4 ($\text{X} = \text{P}, \text{As}, \text{Sb}, \text{Bi}$) compounds: Potential photovoltaic absorbers



K. Bougherara^{a,b}, D.P. Rai^{c,d,*}, A.H. Reshak^{e,f,g,h}

^a Centre de Développement des Technologies Avancées, CDTA - Laser Material Processing Team, PO. BOX 17 Baba-Hassen, Algiers 16303, Algeria

^b Laboratoire d'Etude des Matériaux & Instrumentations Optiques, Faculté des Sciences Exactes, Université Djillali Liabes de Sidi Bel Abbes, Sidi Bel Abbes 22000, Algeria

^c Division of Computational Physics, Institute for Computational Science, Ton Duc Thang University, Ho Chi Minh City, Vietnam

^d Faculty of Electrical and Electronics Engineering, Ton Duc Thang University, Ho Chi Minh City, Vietnam

^e Nanotechnology and Catalysis Research Center (NANOCAT), University of Malaya, Kuala Lumpur 50603, Malaysia

^f Department of Instrumentation and Control Engineering, Faculty of Mechanical Engineering, CTU in Prague, Technicka 4, Prague 6 166 07, Czech Republic

^g Physics department, College of Science, Basrah University, Basrah, Iraq

^h Iraq University College (IUC), Al-Estiqal St., Basrah, Iraq

ARTICLE INFO

Keywords:

FP-LAPW

Mechanical properties

Optoelectronic properties

Photovoltaic absorbers

ABSTRACT

We report a first-principles study of structural, mechanical and optoelectronic properties of the Sn_3X_4 ($\text{X} = \text{P}, \text{As}, \text{Sb}, \text{Bi}$) compounds. The calculations were performed using the full-potential linearized augmented plane wave approach (FP-LAPW). The structural and mechanical properties of Sn_3X_4 ($\text{X} = \text{P}, \text{As}, \text{Sb}, \text{Bi}$) compounds were obtained using GGA-PBE. In addition, The Tran-Blaha modified Becke-Johnson exchange potential (TB-mBJGGA) technique was used to calculate the optoelectronic properties. The calculated electronic band structures and density of states reveal a direct band gap at Γ points varied from 0.11 eV to 1.23 eV for $\text{X} = \text{P}, \text{As}, \text{Sb}, \text{Bi}$. The optical absorption calculations show that all compounds have high absorption coefficients about twenty times greater than that of CuInSe_2 and CdTe in the visible region. The high absorption of these materials could be attributed to the localized p-states of cation ($\text{X} = \text{P}, \text{As}, \text{Sb}, \text{Bi}$) in the lower region of the conduction band.

1. Introduction

The IV_3V_4 ($\text{IV} = \text{C}, \text{Si}, \text{Ge}, \text{Sn}; \text{V} = \text{N}, \text{P}, \text{As}$) family have gained much research interest because of their wide technological applications, incorporating desirable physical properties such as mechanical engineering, photoelectric and photovoltaic applications [1–12]. Through literature review, we have found numerous studies on polymorphs IV_3X_4 compounds, based on first principal calculation. Ahamed et al. [13] investigated the structural, electronic and elastic properties of five crystal phases of Si_3P_4 , i.e., β [P63/m], γ [Fd-3m], pseudocubic [P-42m], Cubic [Im-3m], Cubic-defect [P-43m]. Huang et al. [14], reported the stability and electronic properties of Sn_3P_4 using first-principles calculations of fourteen structures, which includes pseudocubic [p-42m], α

* Corresponding author at: Division of Computational Physics, Institute for Computational Science, Ton Duc Thang University, Ho Chi Minh City, Vietnam.

E-mail address: dibya@tdtu.edu.vn (D.P. Rai).

<https://doi.org/10.1016/j.cjph.2019.03.012>

Received 23 February 2019; Received in revised form 18 March 2019; Accepted 20 March 2019

Available online 10 April 2019

0577-9073/© 2019 Published by Elsevier B.V. on behalf of The Physical Society of the Republic of China (Taiwan).

Table 1

The optimized structural parameters (a , u), independent elastic constants C_{ij} , bulk modulus B , shear modulus G , Young's modulus Y , Poisson ratio ν , anisotropy factor A , Pugh ratio B/G of Sn_3X_4 ($X = \text{P}, \text{As}, \text{Sb}, \text{Bi}$).

Parameters	Sn_3P_4	Sn_3As_4	Sn_3Sb_4	Sn_3Bi_4
$a(\text{\AA})$	5.65	5.87	6.27	6.47
u	0.2841	0.2869	0.2917	0.2899
$C_{11}(\text{GPa})$	91.8	79.9	59.3	53.3
$C_{12}(\text{GPa})$	41.0	34.6	30.1	28.2
$C_{44}(\text{GPa})$	60.7	49.9	37.8	29.7
B (GPa)	57.93	49.70	39.83	36.56
G (GPa)	42.79	36.34	25.81	21.02
Y (GPa)	103.02	87.66	63.68	52.92
ν	0.20	0.21	0.23	0.26
A	0.796	0.793	0.766	0.74
B/G	1.35	1.36	1.54	1.73
C_p	-19.7	-15.3	-7.7	-1.5

[P31c], CaFe_2O_4 [Pnma], Sr_2PbO_4 [Pbam], γ [Fd-3m], Cubic [I-43d], Olivine [Pbnm], $\beta 1$ [P63], CaMn_2O_4 [Pbcm], $\beta 2$ [P63/m], CaTi_2O_4 [Cmcm], Defect-NaCl [Pm-3m], Graphitic [P-6m2], K_2NiF_4 [I4/mmm]. They found that the pseudocubic phase is the most stable phase.

Also Hu et al. [15] studied the structural properties of X_3As_4 properties of X_3As_4 ($X = \text{C}, \text{Si}, \text{Ge}$ and Sn) using ab initio calculations and confirmed that the pseudocubic structure is the most stable phase. Zaikina et al. [16] and Ganesan et al. [17], reported another crystal structure experimentally determined of Sn_3P_4 it crystallizes in the trigonal space group R-3m. and most recently Ruike et al. [18] predicted two novel structures of Sn_3P_4 which crystallizes in tetragonal phase I-42m (121) and orthorhombic phase Pbca (61).

In this paper, we have investigated the elastic, electronic and optical properties of Sn_3X_4 ($X = \text{P}, \text{As}, \text{Sb}$ and Bi) compounds in their cubic defect phases which possesses space group # 215 (P-43m) by means of the first-principles calculations. To the best of our knowledge, no previous theoretical or experimental investigations have been reported yet, except Ahamed et al. report which is cited above for Si_3P_4 . The paper is summarized as the following description. Section 2 briefly describes the computational techniques used in this work. Results and discussions of the structural, elastic, electronic and optical properties, as well as elastic constants, are presented and analyzed in Section 3. Finally, the conclusions are given in details in Section 4.

2. Computational details

The calculations are executed within the first-principles density functional theory framework utilizing the FP-LAPW approach [19], as it is incorporated in the WIEN2k program [20]. The structural and elastic properties are determined using the Perdew-Burke-Ernzerhof generalized gradient approximation (PBE-GGA) [21]. The collected results are listed in Table 1. The optoelectronic properties are calculated using the modified Becke-Johnson exchange potential (TB-mBJGGA) technique developed by Tran and Blaha [22]. TB-mBJGGA have been adopted to derive the better electronic structure. This potential generally gives the value of the band gap in good agreement with the experimental value for simple semiconductors and insulators.

The calculations are carried out using 120 k -points in the IBZ (irreducible Brillouin zone) corresponding to $10 \times 10 \times 10$ in Monkhorst-Pack k -point mesh to compute the total energy. A high density k -grid of $20 \times 20 \times 20$ is used for calculating the electronic and optical properties. A maximum value for partial waves inside atomic spheres of $L_{\text{max}} = 10$ and $K_{\text{max}} = 9/R_{\text{MT}}$, a charge density Fourier-expanded up to $G_{\text{max}} = 14$ Ryd was employed to converge results.

3. Results and discussion

3.1. Structural and elastic properties

The crystal structure of Sn_3X_4 ($X = \text{P}, \text{As}, \text{Sb}, \text{Bi}$) crystallize in the cubic lattice (structure) with space group # 215 (P-43m) and $Z = 1$ as presented in Fig. 1, the unit cell of Sn_3X_4 compounds contains two atoms occupying the positions: Sn on $3d$ (0.5, 0, 0) and X on $4e$ (u, u, u) in Wyckoff coordinates. The predicted structural (lattice parameters, bulk modulus) and elastic properties (elastic constants C_{ij} , shear modulus G , Young's modulus Y , Poisson ratio ν and anisotropy factor A) are summarized in Table 1.

The elastic constants of Sn_3X_4 compounds are calculated by employing homogeneous strain within the framework of linear response theory [23] implemented within the elastic code, to determine the mechanical stability as listed in Table 1. The stability criteria of born [24]:

$$C_{11} > 0; C_{44} > 0; C_{11} > C_{12}; C_{11} + 2C_{12} > 0; C_{11} - C_{12} > 0.$$

are satisfied which means that the Sn_3X_4 compounds are mechanically stable.

Pugh's B/G ratio is a determining factor for ductile or brittle behavior. If B/G ratio is equal to 1.75 or higher, the material is ductile otherwise, the material becomes brittle. The calculated B/G ratio of Sn_3X_4 materials (Table 1) are below 1.75 which means that all the materials are brittle. Another way to evaluate the ductility is Cauchy's pressure ($C_p = C_{12} - C_{44}$) [25]. A positive value

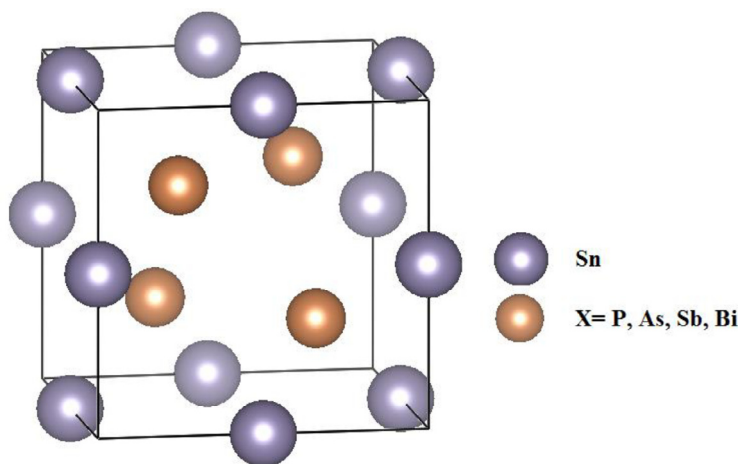


Fig. 1. Crystal structures of the Sn_3X_4 ($\text{X} = \text{P}, \text{As}, \text{Sb}, \text{Bi}$) compounds.

indicates that the material is ductile, whereas a negative value implies its brittleness. The results in Table 1 indicated the brittle behavior for Sn_3X_4 ($\text{X} = \text{P}, \text{As}, \text{Sb}, \text{Bi}$) compounds are in concordance with our previous observation obtained by the Pugh ratio. The elastic anisotropy factor is equal to 1.0 for isotropic materials, while any value larger or smaller than 1.0 indicates anisotropy. It can be seen from Table 1 that the Sn_3Bi_4 compound is more anisotropic than the other compounds.

3.2. Electronic properties

The electronic band structure along the high-symmetry crystallographic direction were calculated by using the TB-mBJ [22] functional for the Sn_3P_4 , Sn_3As_4 , Sn_3Sb_4 and Sn_3Bi_4 compounds. The electronic band structures calculated from TB-mBJ presented in Fig. 2. The results show that the four materials have direct energy band gaps where the VBM (valence band maxima) and the CBM (conduction band minima) are at the Γ point of the Brillouin zone. The calculated direct band gaps are 1.23 eV (Sn_3P_4), 0.85 eV (Sn_3As_4), 0.22 eV (Sn_3Sb_4) and 0.11 eV (Sn_3Bi_4). One can see that the width of the bandgap decreases with moving from P to Bi. The bandgap reduction could be attributed to shift of the conduction band towards the Fermi level (E_F) when one move from P to Bi. Importantly, semiconductor compounds with direct band gap are optically active and can have wide technological applications in the optoelectronic and photonic devices. Especially, the materials with direct band gap and highest-energy valence bands (VBs) at the Γ point are most favourable for fabrication in optoelectronic devices.

We have also calculated the total density of states (TDOS) and the partial density of state (PDOS) of Sn_3X_4 ($\text{X} = \text{P}, \text{As}, \text{Sb}, \text{Bi}$) compounds by using TB-mBJ. The calculated TDOS and PDOS are plotted over an energy range from -8 eV to 4 eV [see Fig. 3]. The low-lying valence bands ranging from approximately -7.5 to -4.0 eV are mainly composed of localized s states of Sn atom, and s and p states of X (P, As, Sb, Bi) atoms. The valence bands ranging from -4.0 eV up to the Fermi level are mainly populated by p orbitals of Sn and X atoms. The conduction bands close to the Fermi level are mainly formed by p states of Sn atom with s and p states of X atoms.

3.3. Optical properties

The optical properties of Sn_3X_4 ($\text{X} = \text{P}, \text{As}, \text{Sb}, \text{Bi}$) compounds are calculated using TB-mbj approximation and plotted for an incident photon energy up to 20 eV. Fig. 4 shows the variation of the optical parameters like the dielectric functions which are derived from the Ehrenreich and Cohen's equation $\varepsilon(\omega) = \varepsilon_1(\omega) + i\varepsilon_2(\omega)$ [26], where $\varepsilon_1(\omega)$ is the real part of dielectric function $\varepsilon_1(\omega)$ and $\varepsilon_2(\omega)$ the imaginary part. From Fig. 4, we have noticed that the static dielectric constant $\varepsilon_1(0)$ for Sn_3P_4 , Sn_3As_4 , Sn_3Sb_4 and Sn_3Bi_4 are 12.64, 15.38, 23.65 and 26.12 respectively. Following these values, one can conclude that the value of the dielectric constant shifts to high value when we substitute P by As, As by Sb and Sb by Bi atoms. This could be explained following Penn model [27], which describe the relationship between the band gap E_g and $\varepsilon_1(0)$. Which implies that the compound with the smaller energy gap E_g has a larger $\varepsilon_1(0)$. Furthermore, the $\varepsilon_1(\omega)$ spectra show main peaks at about 18.31 eV, 21.71 eV, 29.93 eV and 31.20 eV for Sn_3P_4 , Sn_3As_4 , Sn_3Sb_4 and Sn_3Bi_4 , respectively.

Other optical constants, like absorption coefficient $\alpha(\omega)$, reflectivity $R(\omega)$, and refractive index $n(\omega)$, can be derived from $\varepsilon_1(\omega)$ and $\varepsilon_2(\omega)$ [28]. The absorption coefficient is an important criterion to evaluate the optical response of a material. The absorption spectra are shown in Fig. 5 in comparison with other PV materials (GaAs, CdTe and CuInSe₂). Our calculated absorption coefficient spectra for the investigated compounds show that these materials have good optical absorption, twenty times larger than that of CuInSe₂, CdTe and GaAs. With a higher value for Sn_3Bi_4 and Sn_3Sb_4 in visible range which makes them suitable for photovoltaic absorbers. The High absorption of these materials could be explained by the localized p-states of cation ($\text{X} = \text{P}, \text{As}, \text{Sb}, \text{Bi}$) present in the inferior region of the conduction band.

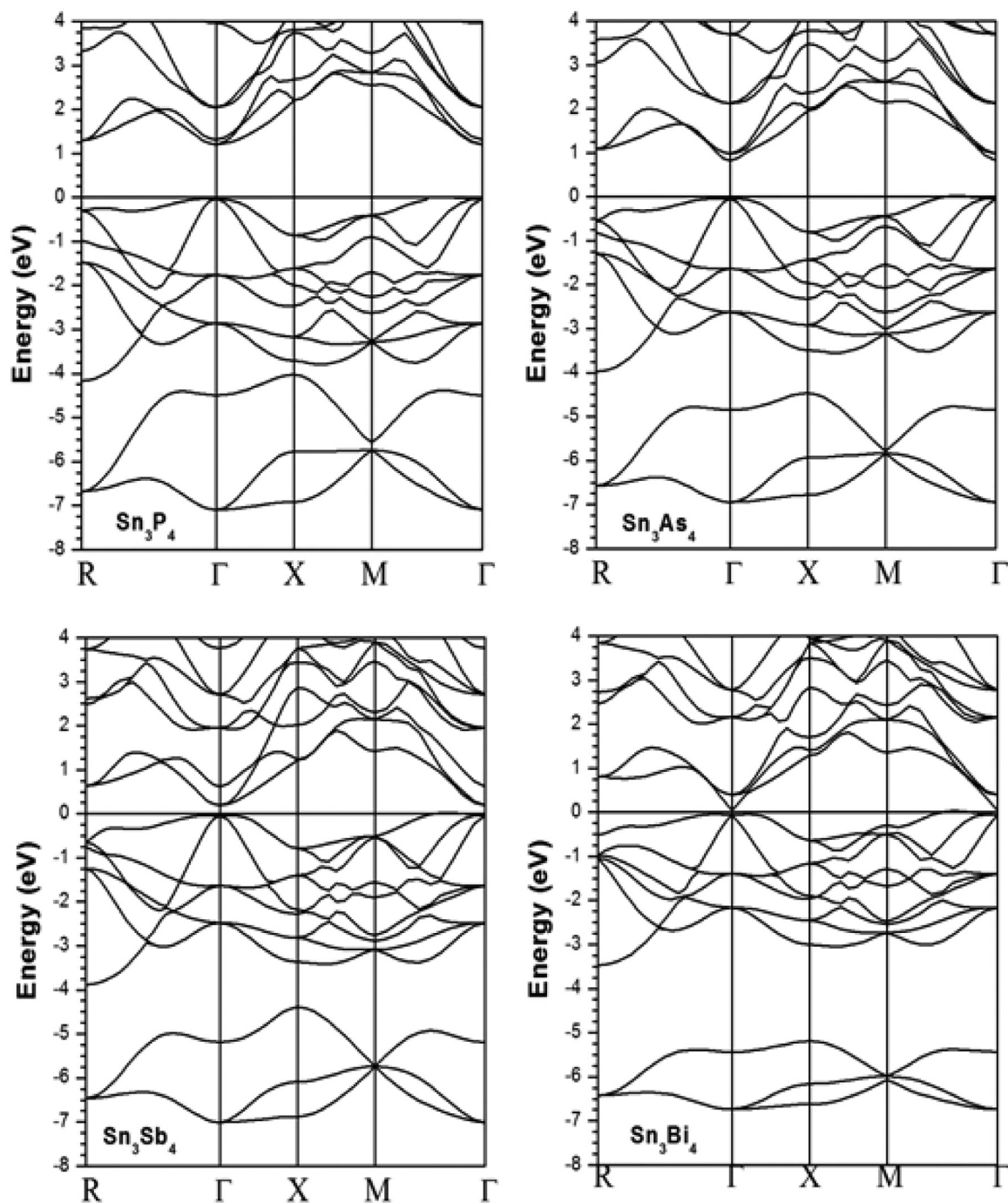


Fig. 2. Band structures of Sn_3P_4 , Sn_3As_4 , Sn_3Sb_4 and Sn_3Bi_4 using PBE-GGA + mBJ.

The calculated reflectance spectra of Sn_3X_4 compounds are plotted in Fig. 6. The reaction at zero frequency reactivity, $R(0)$, is found to be relatively at a high value, 0.31, 0.35, 0.43 and 0.45 for Sn_3P_4 , Sn_3As_4 , Sn_3Sb_4 and Sn_3Bi_4 respectively.

From above we concluded that the calculated electronic properties, show a direct band gap (Γ - Γ) for Sn_3X_4 ($X = \text{P}, \text{As}, \text{Sb}, \text{Bi}$) compounds with a gap ranging from 0.1 eV to 1.22 eV. Furthermore, we found that these materials have a strong absorption coefficient ($>10^5 \text{cm}^{-1}$) in the visible region twenty times larger than that of CuInSe_2 , CdTe and GaAs . Also have greater refractive indices than the that of CuInSe_2 , CdTe and GaAs which indicate potential applications of these compounds in solar cell devices as well as in optoelectronic devices.

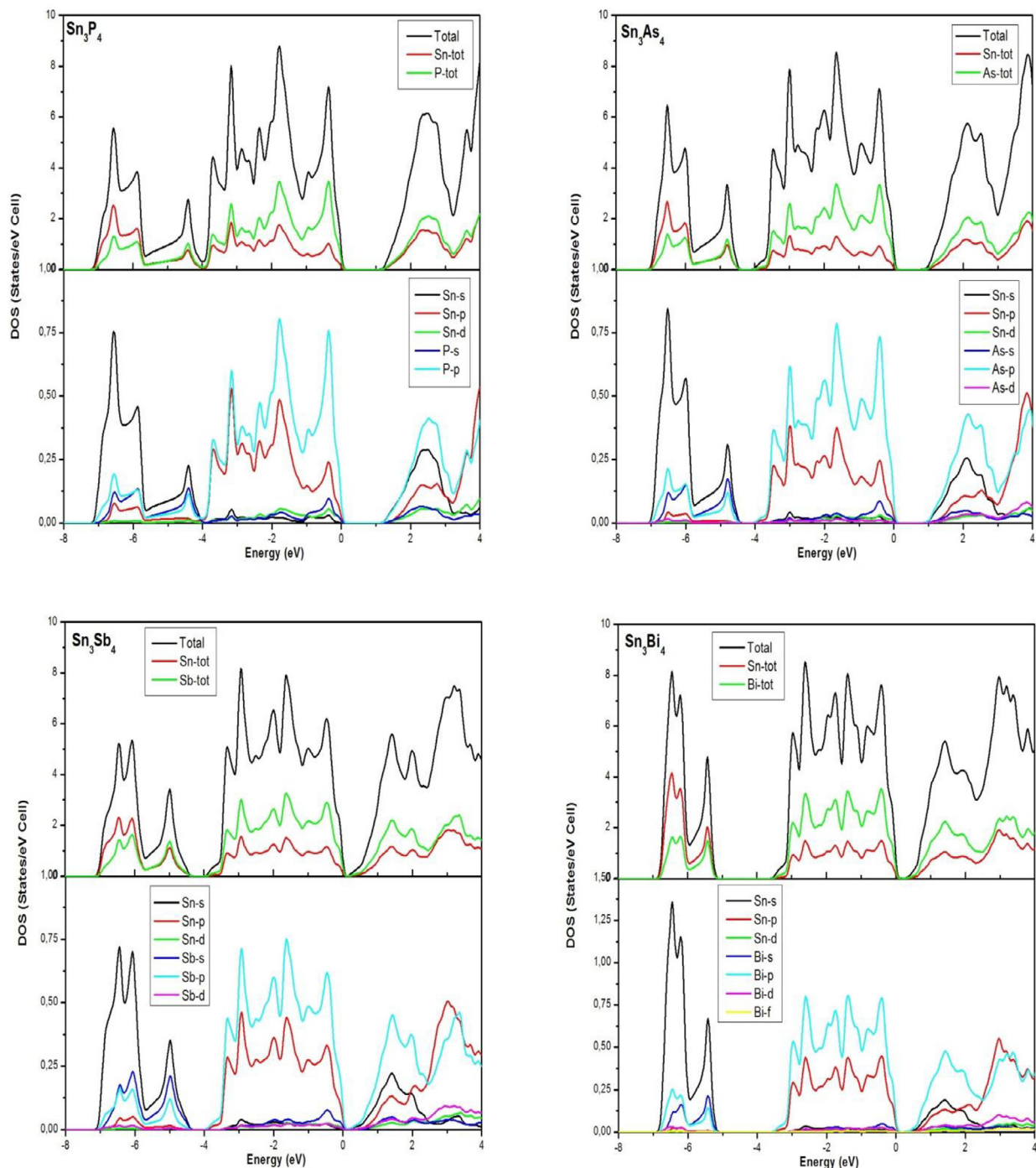


Fig. 3. The calculated partial and total density of states (DOS) for Sn_3P_4 , Sn_3As_4 , Sn_3Sb_4 and Sn_3Bi_4 using PBE-GGA + mBJ.

4. Conclusion

We performed detailed investigation on the structural, elastic and optical properties of semiconductor materials Sn_3P_4 , Sn_3As_4 , Sn_3Sb_4 and Sn_3Bi_4 using first-principles FP-APW + lo method within GGA-PBE and TB-mBJ functional. We first calculated the structural and elastic properties. Our calculation predicts a mechanical stability and brittle behavior for all the four compounds. We then calculated the electronic properties, which predict a direct band gap for the four compounds at the Γ points with a gap ranging from 0.1 eV to 1.22 eV. Lastly, we determined the optical properties of these compounds and found that they have strong absorption coefficient ($> 10^5 \text{ cm}^{-1}$) in the visible region, twenty times larger than that of CuInSe_2 , CdTe and GaAs compounds. Also it shows

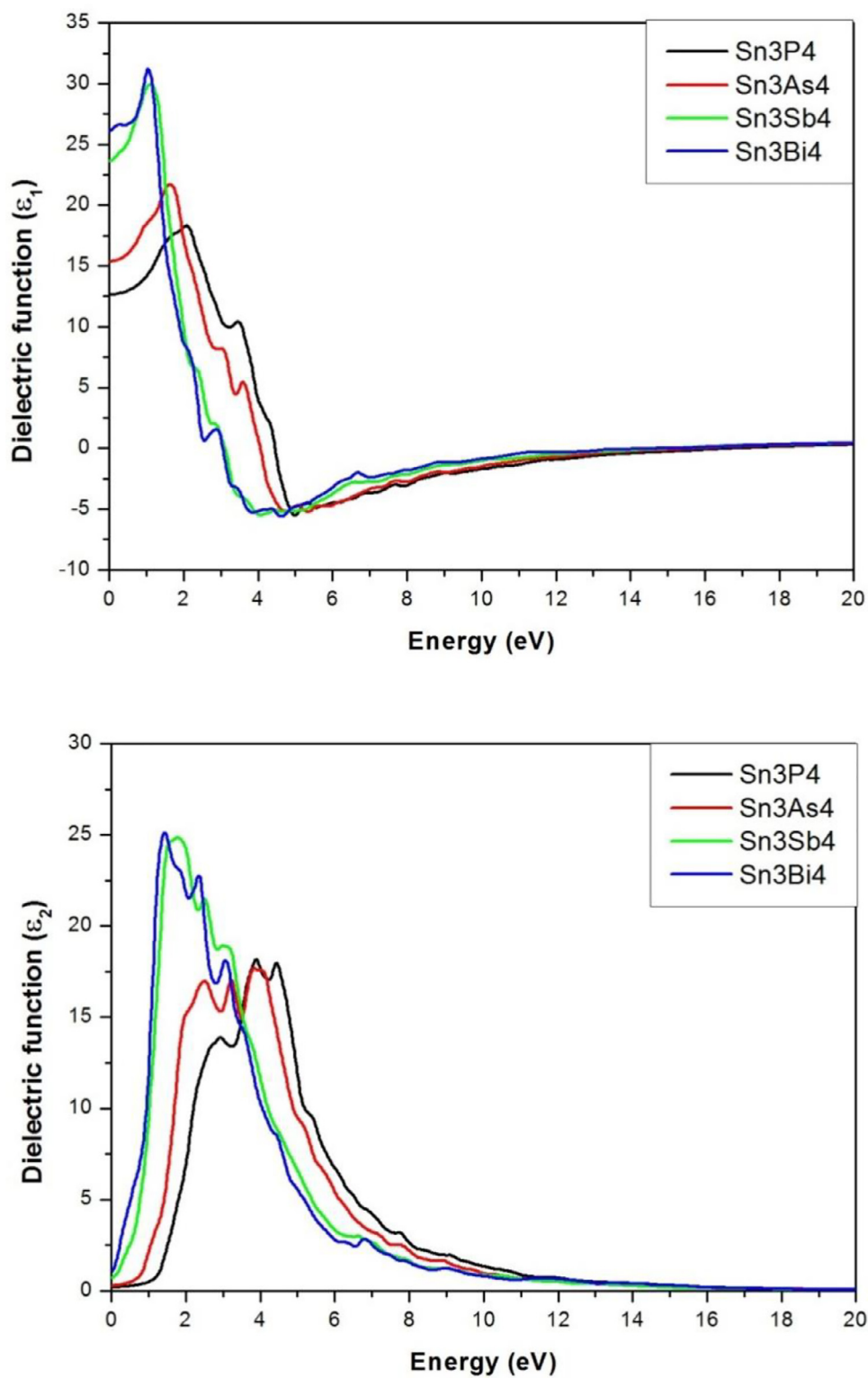


Fig. 4. The calculated real $\epsilon_1(\omega)$ and imaginary $\epsilon_2(\omega)$ parts of complex dielectric constant for Sn_3P_4 , Sn_3As_4 , Sn_3Sb_4 and Sn_3Bi_4 using PBE-GGA+mBJ.

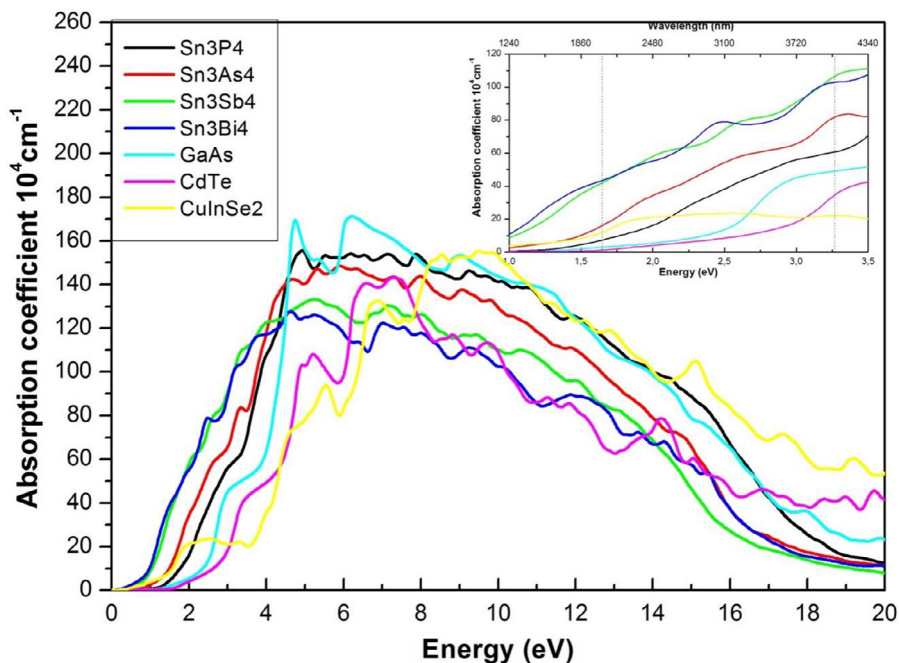


Fig. 5. The calculated absorption coefficient of Sn_3X_4 ($x = \text{P}, \text{As}, \text{Sb}, \text{Bi}$) using PBE-GGA + mBJ compared with those of GaAs, CdTe and CuInSe_2 . The vertical lines correspond to the visible spectrum range.

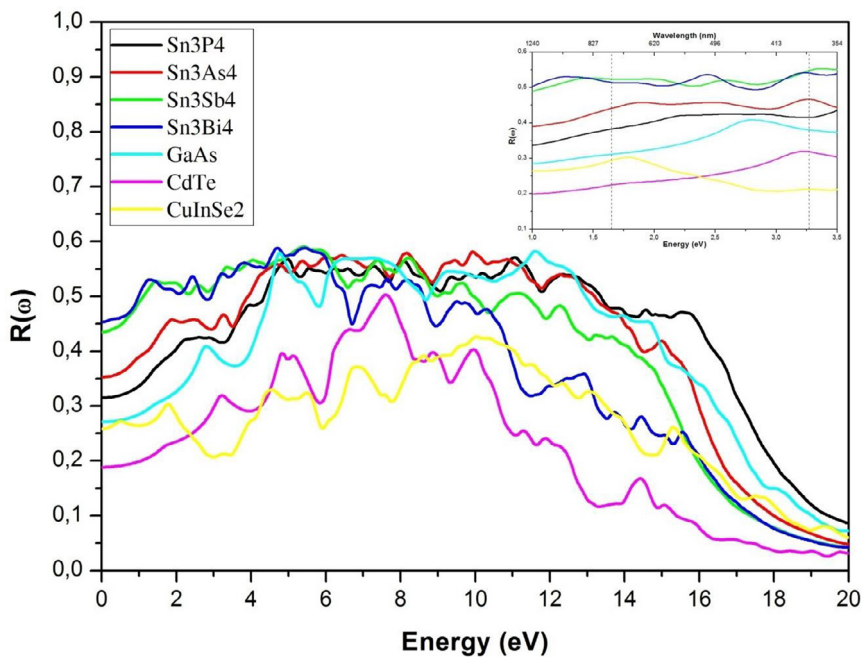


Fig. 6. The calculated reflectance spectra of Sn_3X_4 ($x = \text{P}, \text{As}, \text{Sb}, \text{Bi}$) using PBE-GGA + mBJ compared with those of GaAs, CdTe and CuInSe_2 . The vertical lines correspond to the visible spectrum range.

greater refractive indices than the that of CuInSe_2 , CdTe and GaAs which indicate potential applications of these compounds in solar cell devices.

Acknowledgments

The Computations were performed on the Cloud Computing System provided by CDTA and the Al-Farabi Cluster computer of the

Ecole Nationale Polytechnique Oran - MAURICE AUDIN.

References

- [1] K.D. Pham, N.N. Hieu, H.V. Phuc, I. Fedorov, C. Duque, B. Amin, C.V. Nguyen, *Appl. Phys. Lett.* 113 (17) (2018) 171605.
- [2] P.T.T. Le, N.N. Hieu, L.M. Bui, H.V. Phuc, B.D. Hoi, B. Aming, Ch.V. Nguyen, *Phys. Chem. Chem. Phys.* 20 (2018) 27856.
- [3] D.Q. Khoa, C.V. Nguyen, H.V. Phuc, V.V. Ilyasov, T.V. Vu, N.Q. Cuong, B.D. Hoi, D.V. Lu, E. Feddi, M. El-Yadri, M. Farkous, N.N. Hieu, *Phys. B Condens. Matter* 545 (2018) 255–261.
- [4] M.L. Cohen, *Phys. Rev. B* 32 (1985) 7988.
- [5] Y. Zhang, T. Mori, J. Ye, M. Antonietti, *J. Am. Chem. Soc.* 132 (2010) 6294.
- [6] Y. Zhang, M. Antonietti, *Chem. Asia J.* 5 (2010) 1307.
- [7] F.L. Riley, *J. Am. Ceram. Soc.* 83 (2000) 245.
- [8] Q. Hua, J. Rosenberg, J. Ye, E.S. Yang, *J. Appl. Phys.* 53 (1982) 8969.
- [9] D.B. Alford, L.G. Meiners, *J. Electrochem. Soc.* 134 (1987) 979.
- [10] I. Honma, H. Kawai, H. Komiyama, K. Tanaka, *J. Appl. Phys.* 65 (1989) 1074.
- [11] G.A. Johnson, V.J. Kapoor, *J. Appl. Phys.* 69 (1991) 3616.
- [12] I. Chambouleyron, A.R. Zanatta, *J. Appl. Phys.* 84 (1998) 1.
- [13] A.S. Ahamed, H. Chen, *J. Southwest Univ.* 29 (2007) 1.
- [14] M. Huang, Y.P. Feng, Stability and electronic properties of Sn3P4, *Phys. Rev. B* 70 (2004) 3352–3359.
- [15] C. Hu, Y.P. Feng, *Phys. Rev. B* 74 (2006) 104102.
- [16] J.V. Zaikina, K.A. Kovnir, A.N. Sobolev, I.A. Presniakov, V.G. Kytin, V.A. Kulbachinskii, A.V. Olenov, O.I. Lebedev, G. Van Tendeloo, E.V. Dikarev, A.V. Shevelkov, *Chem. Mater.* 20 (2008) 2476–2483.
- [17] R. Ganesan, K.W. Richter, C. Schmetterer, H. Effenberger, H. Ipsier, *Chem. Mater.* 21 (2009) 4108–4110.
- [18] Y. Ruike, M. Yucan, W. Qun, Z. Dongyun, *Chin. J. Phys.* 56 (2018) 886.
- [19] D.J. Singh, L. Nordstrom, *Planewaves Pseudopotentials and the LAPW Method*, 2nd ed., Springer, Berlin, 2006.
- [20] P. Blaha, K. Schwarz, G. Madsen, D. Kvasnicka, J. Luitz, *WIEN2k, An Augmented Plane Wave Local Orbitals Program for Calculating Crystal Properties*, Vienna University of Technology, Austria, 2001.
- [21] J.P. Perdew, K. Burke, M. Ernzerhof, *Phys. Rev. Lett.* 77 (1996) 3865.
- [22] F. Tran, P. Blaha, *Phys. Rev. Lett.* 102 (2009) 226401.
- [23] R. Golezorkhtabara, P. Pavone, J. Spitaler, P. Puschnig, C. Draxl, *Comp. Phys. Commun.* 184 (2013) 1861.
- [24] M. Born, K. Huang, *Dynamical Theory of Crystal Lattices*, Clarendon, Oxford, 1954.
- [25] D.G. Pettifor, Theoretical predictions of structure and related properties of intermetallics, *Mater. Sci. Technol.* 8 (4) (1992) 345–349.
- [26] K. Bougherara, F. Litimein, R. Khenata, E. Uçgun, H.Y. Ocak, S. Ugur, G.U gur, A.H. Reshak, F. Soyalt, S. Bin-Omran, *Sci. Adv. Mater.* 5 (2013) 97–106.
- [27] D.R. Penn, *Phys. Rev.* 128 (1962) 2093.
- [28] S. Saha, T.P. Sinha, A. Mookerjee, *Phys. Rev. B* 62 (2000) 8828.